Nontidal Ocean Loading Observed by VLBI Measurements

## D. S. MacMillan and D. Eriksson

NVI, Inc.

Introduction

Vertical deformation due to nontidal ocean loading is large enough to be seen in VLBI geodetic parameter estimates. Typical peak-to-peak vertical variations are 4-6 mm at VLBI sites. At VLBI sites, the loading signal has an annual character, but as with atmospheric and hydrological loading, we also observe interannual variations. These variations are caused by temporal variations of the geographic distribution of ocean surface mass. Here, we report on our calculation of the mass loading derived from JPL Estimation the Circulation and Climate of the Ocean (ECCO) model ocean bottom pressure estimates from 1993 to 2009. To do this, we evaluated the convolution of Farrell's loading Green's function with the ocean loading mass field, given by a global grid of ECCO model bottom pressures. We investigated the reduction in baseline length, site position scatter, and site vertical annual amplitudes when nontidal ocean loading is applied in VLBI analysis.

1 Nontidal Ocean Data

Vertical and horizontal nontidal ocean loading is computed using the ECCO ocean model maintained at Jet Propulsion Laboratory (JPL). The model is described by Fukumori [2002]. The ECCO model is available on a latitude/longitude grid with 224 latitudes and 360 longitudes where the latitude range is -80 to +80 degrees with a 12-hour time resolution. Data is available since 1993 and has a latency of about 3 weeks. The model conserves oceanic volume but is not mass.conserving.

RMS variation of the 12h OBP in the ECCO model, 1993-2009
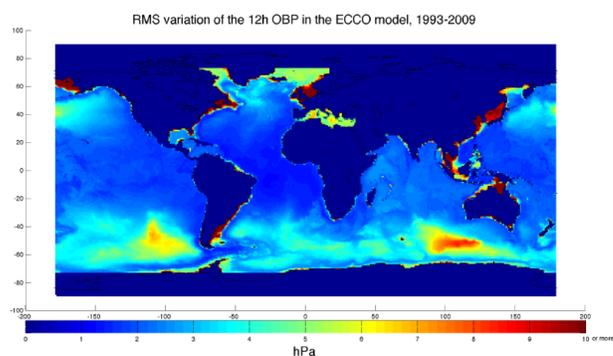
It can be seen in the above figure that the RMS variation of bottom pressure is largest for coasts. The variations are much smaller than variations observed for atmospheric pressure loading. Therefore, we expect smaller loading displacements of a several millimeters. Coastal sites will experience much stronger loading signals than inland sites.
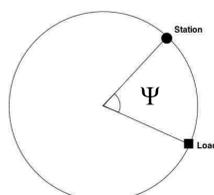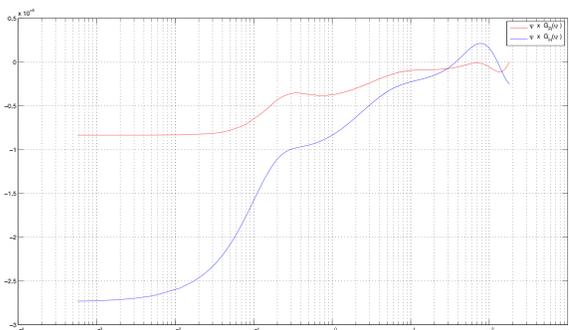
2 The Green's Function Approach

According to Farrell (1972), the displacement at a point with longitude/latitude coordinates (λ, φ) due to a mass loading distribution $\Delta m(\vec{r}')$ is given by:

- Vertical: $$u_R(\vec{r}) = \iint_S \Delta m(\vec{r}') G_R(\psi) \cos(\phi') d\lambda' d\phi'$$

-- East-West: $$u_{EW}(\vec{r}) = \iint_S \Delta m(\vec{r}') \sin(A) G_H(\psi) \cos(\phi') d\lambda' d\phi'$$

-- North-South: $$u_{NS}(\vec{r}) = \iint_S \Delta m(\vec{r}') \cos(A) G_H(\psi) \cos(\phi') d\lambda' d\phi'$$

A=azimuth from local North to load direction

(Blue) Logarithmic plot of $\psi\, G_R(\psi)$
(Red) Logarithmic plot of $\psi\, G_H(\psi)$

The loading Green's function is the response at the station due to a mass load at an angular distance ψ from the station. The closer the mass is to the station, the larger the response. By integrating over the surface of the earth, we will get the total adjustment of the station position caused by the surface mass distribution. The loading contribution is dominated by loading near the station as well as any large coherent regional loads far from the station.

## 3 Nontidal Ocean Loading Displacement Series

MATERA

TSUKUBA32
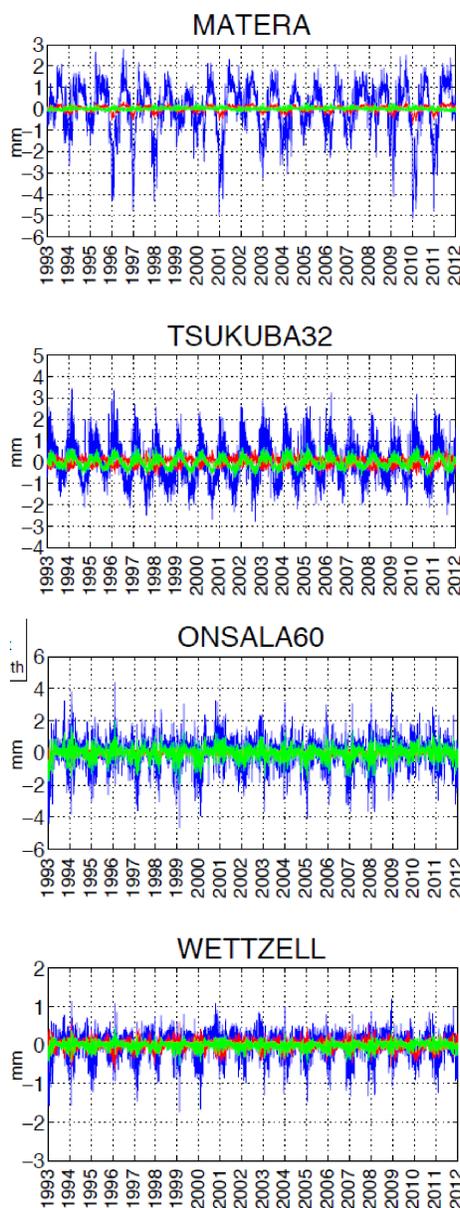
ONSALA60

WETTZELL

Up (blue) , East (red) , North (green)

The figures above shows some typical loading series from the ECCO data period (1993-2009). The loading series shown are for the four sites Matera (Italy), Onsala (Sweden), Tsukuba (Japan), and Wettzell (Germany. The first three are coastal sites in areas where we saw a large variation in the ECCO bottom pressure data, while Wettzell is an inland site. We therefore expect the loading series for Wettzell to have a much smaller variance than the coastal sites. The signals for Tsukuba and Matera are clearly seasonal. It is also clear that the 3-dimensional loading displacements are predominantly in the vertical direction. Generally peak-to-peak loading displacements at VLBI coastal sites are 4-6 mm in the vertical and less than 1 mm in the horizontal.

4 Annual Variation of Vertical Loading

We ran two terrestrial reference frame solutions, where station positions, velocities, and annual site position amplitudes were estimated globally. In the first solution, hydrology loading series generated using GLDAS data [Rodell et al., 2004] were applied. In the second solution, nontidal ocean loading was also applied. As shown below, there was a reduction in the vertical annual amplitude for most of the coastal VLBI sites.
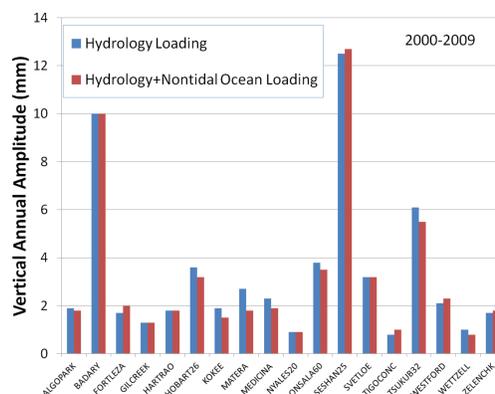
5 Reduction of Variance in VLBI Analysis

We applied our loading series in standard Calc/Solve VLBI analysis to determine whether our solution site postion estimates were improved. We ran two solutions to estimate daily site positions for the sites in our weekly operational R1 and R4 networks from 2003-2009: 1) No nontidal ocean loading applied and 2) ECCO loading series applied

R1R4, 2003–2009, sessions with 50 or more observations

Vertical, R1R4, 2003-2009
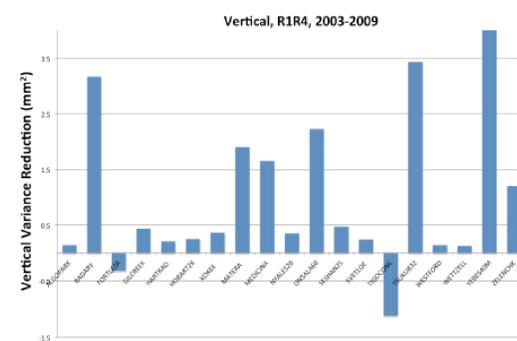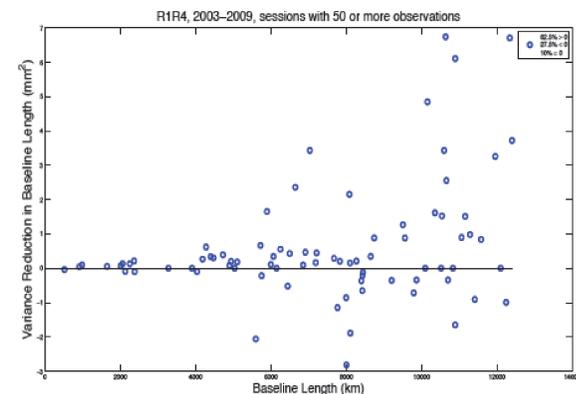
(a) After applying the ECCO loading corrections. 60% of the baselines show positive reduction in variance. We included all baselines including baselines with non-coastal sites, where the nontidal loading signal is small

(b) The variance of vertical position estimates is reduced for most sites. The position estimates are improved most for coastal stations where the nontidal ocean loading signal is strongest., although Forteleza (Brazil) shows no improvement.

Conclusions and Future Work

-- Ocean bottom pressures have the largest variation near coasts

-- Applying the ECCO nontidal ocean loading series reduces VLBI vertical scatter for most sites

-- Baseline length scatter is reduced for 60% of the VLBI baselines when nontidal ocean loading is used (baselines with non-coastal sites included)

-- Nontidal ocean loading modeling reduces the annual vertical amplitudes for most coastal sites

-- We have developed a service to provide a 12-hr nontidal ocean loading series for all VLBI sites from 1993 to the present:

http://lacerta.gsfc.nasa.gov/oclo

References

Farrell, W. E., Deformation of the earth by surface loads. *Rev. Geophys. and Spac. Phys.*, 10(3):761–797, 1972.

Fukumori, I, A partitioned Kalman filter and smoother, *Mon. Weather Rev.*, 130, 1370-1383, 2002.

Rodell, M., P. R. Houser, U. Jambor, J. Gottschalck, K. Mitchell, C.-J. Meng, K. Arsenault, B. Cosgrove, J. Radakovich, M. Bosilovich, J. K. Entin, J. P. Walker, D. Lohmann, and D. Toll, The Global Land Data Assimilation System, *Bull. Amer. Meteor. Soc.*, 85(3), 381-395, 2004.